DMT and harmine responses in monocyte-derived microglia-like cells from patients with treatment-resistant depression

Online Resource 1 Supplementary material

Journal of Neural Transmission

Francisco Cid Coelho Pinto, Fátima de Cássia Evangelista de Oliveira, Hilda Tahim de Souza, José de Brito Vieira Neto, Isabelle de Fátima Vieira Camelo Maia, Sérgio André de Souza Júnior, Adriano José Maia Chaves Filho, Fábio de Oliveira Silva Ribeiro, Alyne Rodrigues de Araujo Nobre, Claudio Costa dos Santos, Islay Lima Magalhães, Caio Andrade de Oliveira, Deysi Viviana Tenazoa Wong, Claudia do Ó Pessoa, David Freitas de Lucena, Maria Francilene Souza Silva, Danielle S. Macedo

Corresponding author: Danielle S. Macedo. Department of Physiology and Pharmacology, Federal University of Ceará, Fortaleza, Brazil. E-mail: danielle.macedo@ufc.br

Supplementary Methods

S1. Membrane-integrity assessment by propidium iodide

Membrane integrity was assessed independently by propidium iodide (PI) staining. Following the indicated experimental treatments, cells were resuspended in 100 µL of binding buffer, and 5 µL of propidium iodide solution (0.5 mg/mL) was added. Samples were incubated for 15 min protected from light, followed by addition of 400 µL of binding buffer before acquisition on a Thermo Fisher Scientific Attune flow cytometer. Corresponding unstained controls were used to establish fluorescence boundaries. Acquisition and gating are described in Supplementary Methods S4. Results were expressed as the percentage of PI-positive events within the gated population of interest, indicating compromised plasma-membrane integrity.

S2. Panoptic staining-based morphological assessment

iMGs from two healthy-control donors (HC01 and HC02) were plated on circular coverslips in 24-well plates at 5 × 10^5 cells/mL. Cells received LPS (100 ng/mL) for 24 h followed by DMT (90 µg/mL) or harmine (35 µM) for 3 h. Coverslips were processed with a rapid Panoptic kit (Laborclin, Brazil): 0.1% triarylmethane for 10 s, 0.1% xanthene dyes for 20 s, and 0.1% thiazine dyes for 20 s. Slides were rinsed with distilled water, dried, mounted with Entellan, and examined using a Nikon Eclipse Ti microscope with a 20× objective. Process number, process length, and cell-body morphology were described with reference to published morphological categories (Bruzelius et al. 2021), without assigning functional inflammatory states. Cells were nested within donors and were not treated as independent biological replicates. These exploratory observations were separate from the principal pharmacological assays in TRD-derived iMGs.

S3. Exploratory atomic force microscopy

Cell-surface topography was examined by atomic force microscopy (TT-AFM, AFM Workshop, USA) in intermittent-contact mode using silicon probes (TAP300-G, Ted Pella; resonance frequency 262.64 kHz) at 512 × 512-pixel resolution. Image processing and analysis were performed in Gwyddion 2.63. Outputs included three-dimensional surface reconstructions, two-dimensional height and amplitude maps, and surface profiles of texture, waviness, and roughness. Arithmetic mean surface roughness (Ra) was extracted from 1.88 × 1.88 µm regions of interest. For TRD02, 60 regions were analyzed per experimental condition. For TRD03, 130 regions were analyzed per experimental condition, with all region-level

observations retained in the final descriptive analysis. Because AFM data were available from only two patients, regions and cells were treated as nested technical measurements and were not considered independent biological replicates. AFM findings were therefore interpreted separately by donor, and the complete representative image sets are presented in Supplementary Figs. S2 and S3.

S4. Flow cytometry acquisition and analysis

Flow cytometry was performed using an Attune™ NxT Flow Cytometer (Thermo Fisher Scientific). iMGs were resuspended in BSA-containing buffer and incubated for 30 min with the indicated antibodies. CD11b-FITC and CD45-PE were analyzed by double staining, whereas CD200 and TMEM119 were evaluated in separate tubes. For CD11b/CD45 characterization, pooled aliquots generated from the experimental conditions were used to prepare unstained, CD11b-FITC single-stained, CD45-PE single-stained, and CD11b-FITC/CD45-PE double-stained controls. Unstained and single-stained controls were used to assess background fluorescence, establish fluorescence boundaries, and perform FITC/PE compensation. A target of 10,000 events per sample was set. When cell availability was insufficient to reach this target, acquisition continued until the available cell suspension was exhausted, yielding approximately 2,000–10,000 acquired events per sample.

CD86 was assessed using a PE-Cyanine7-conjugated monoclonal antibody (clone GL1, Thermo Fisher Scientific/Invitrogen eBioscience, cat. no. 25-0862-82). Data were analyzed using Floreada.io. The population of interest was first identified using forward-scatter (FSC) and side-scatter (SSC) parameters to exclude debris, after which marker expression was evaluated within the gated population. For CD11b/CD45 analyses, bivariate plots were used and the same compensation and gating strategy was applied consistently across experimental conditions. Corresponding unstained controls were used for the independent CD200, TMEM119, CD86, and PI analyses to establish fluorescence boundaries. Marker positivity was expressed as the percentage of positive events within the gated population. Flow-cytometry events were considered nested measurements within each donor sample and were not treated as independent biological replicates. Representative CD11b/CD45 plots and unstained controls are shown in Supplementary Fig. S1.

S5. Immunofluorescence reagent details

For IBA1 immunolabeling, cells were incubated with goat polyclonal anti-IBA1 antibody (Santa Cruz Biotechnology, cat. no. sc-28530), followed by a donkey anti-goat IgG H&L secondary antibody conjugated to Alexa Fluor 488 (Abcam, cat. no. ab150129).

Experimental-unit definition. The donor was the biological replicate. Wells, slides, fields, cells, flow-cytometry events, and AFM regions were technical or nested observations. Available replicate measurements were summarized within donor and condition before inference.

S6. Astrocyte culture and concentration-selection assays

An immortalized mouse astrocyte line provided by a collaborating group at the Federal University of São Paulo (UNIFESP) was cultured in Dulbecco's Modified Eagle Medium (DMEM) with 10% fetal bovine serum (FBS) and 1% antibiotics at 37°C under 5% CO_2. At approximately 80% confluence, cells were detached with 0.05% trypsin in 0.53 mM EDTA and counted by Trypan blue exclusion using a Neubauer chamber. Seeding densities were 5×10^5 cells/mL in 12- or 24-well plates and 1×10^5 cells/mL in 96-well plates, depending on the assay.

Preliminary concentration–response assays guided concentration selection for subsequent iMG experiments; they were not designed to establish microglia-specific safety or clinically relevant exposure.

Astrocyte metabolic activity was assessed by MTT assay (Mosmann 1983; Denizot and Lang 1986) after DMT exposure (0.78–800 µg/mL; 24, 48, or 72 h) or harmine exposure (1.56–200 µM; 24 or 48 h). Cells were incubated with MTT (5 mg/mL) for 3 h, formazan was solubilized in DMSO, and absorbance was measured at 595 nm. Results were normalized to the untreated control as an indirect viability measure. Experiments were independently repeated three times with duplicate wells per condition. These exposure periods refer to astrocyte screening; iMG drug exposure was 3 h for both compounds (Section 2.5).

Additional viability screening was performed in peripheral blood mononuclear cells (PBMCs) using the Alamar Blue assay (O'Brien et al. 2000), with fluorescence measured at 560/590 nm. Half-maximal inhibitory concentration (IC_{50}) values and corresponding 95% confidence intervals were estimated by nonlinear regression using a four-parameter logistic model in GraphPad Prism (version 10.4.1).

Limited primary-cell yield precluded donor-specific concentration–response testing. DMT (90 µg/mL) and harmine (35 µM) were selected below the screening IC_{50} estimates, which do not establish equivalent sensitivity or absence of toxicity in human iMGs. Membrane integrity was assessed separately by propidium iodide (PI) staining in available iMG preparations (Supplementary Methods S1).

Supplementary Results

S1. Membrane integrity assessed by propidium iodide (n = 4 patients)

PI positivity varied among the four TRD donors. LPS-associated increases occurred in some donors, and neither DMT nor harmine showed a consistent additional increase relative to LPS alone. With four donors and one missing treatment measurement, these observations were interpreted descriptively and do not establish absence of membrane damage or other forms of toxicity.

S2. Panoptic staining-based morphological assessment (n = 2 healthy controls, HC01 and HC02)

Panoptic images from HC01 and HC02 showed more rounded, less process-bearing profiles after LPS and more elongated, process-bearing profiles after DMT or harmine (Supplementary Fig. S4). These qualitative observations do not establish a treatment-specific morphological effect, functional recovery, or a difference between healthy-control and TRD-derived cells.

S3. Exploratory atomic force microscopy (n = 2 patients, TRD02 and TRD03)

AFM data from TRD02 and TRD03 showed donor-dependent roughness patterns. Mean Ra values for control, LPS, LPS + DMT, and LPS + HRM were 199.3, 201.8, 215.3, and 243.9 nm in TRD02, and 91.90, 96.22, 82.62, and 90.79 nm in TRD03. All 130 regions per condition were retained for TRD03. Because the directions of change differed between donors and regions were nested technical observations, results were described separately by donor without pooled inference (Supplementary Figs. S2 and S3).

S4. Clinical characterization

The clinical cohort comprised HC01–HC04 and TRD01–TRD07. Assay participation and exclusions are detailed in Supplementary Table S1.

Mean age was 36.00 ± 7.62 years in healthy controls and 35.86 ± 13.95 years in patients with TRD (Mann–Whitney U = 17, exact permutation p = 0.6121). Sex distribution (Fisher's exact p = 0.2424) and family psychiatric history (Fisher's exact p = 0.5758) also did not differ statistically between groups; given the small sample size, these findings should not be interpreted as demonstrating group comparability. Mean illness duration in the TRD group was 6.43 ± 3.51 years.

As expected from the recruitment criteria, patients with TRD had substantially higher depressive symptom severity than healthy controls. Mean MADRS total scores were 40.29 ± 5.15 in the TRD group, and 3.50 ± 1.29 in healthy controls (Mann–Whitney U = 0, exact permutation p = 0.0061; Supplementary Table S4 and Supplementary Fig. S5). MADRS item-level profiles are shown in Supplementary Fig. S5A.

S5. Concentration-selection results

Astrocyte metabolic activity decreased predominantly at higher concentrations (Supplementary Fig. S6). DMT IC_{50} estimates were 259.0 µg/mL at 24 h (95% CI, 185.4–397.5), 216.6 µg/mL at 48 h (180.6–262.9), and 255.6 µg/mL at 72 h (198.8–341.8). Estimates did not decrease monotonically with exposure duration; time points were not formally compared.

For harmine, the estimated IC_{50} was 112.5 µM at 24 h (95% CI, 110.0–122.2) and 84.71 µM at 48 h (95% CI, 70.98–100.6). Harmine was not evaluated at 72 h.

PBMC 24-h IC_{50} estimates were 184.9 µg/mL for DMT (95% CI, 167.1–203.8) and 112.6 µM for harmine (83.17–164.4). Estimates from three independent experiments performed in duplicate are summarized in Supplementary Table S2.

The selected iMG concentrations, DMT 90 µg/mL and harmine 35 µM (Supplementary Table S5), were below these screening estimates. Descriptive PI observations did not show a consistent treatment-associated increase beyond LPS alone, but do not establish absence of toxicity (Supplementary Results S1).

S6. Differentiation and phenotypic characterization

Brightfield imaging documented progressive morphological changes during differentiation, with cells becoming increasingly adherent, elongated, and process-bearing between culture days 1 and 13 (Supplementary Fig. S7A).

$CD11b^{+}CD45^{+}$ proportions increased from 16.7% in PBMCs to 82.2% in iMGs for HC02 and from 15.1% to 55.4% for HC03. Corresponding values were 0.0% to 72.8% for TRD02 and 0.0% to 71.6% for TRD03 (Supplementary Fig. S7B).

These observations are consistent with myeloid enrichment during differentiation but do not establish resident microglial identity.

TRD03 showed 42.8% positivity in the no-antibody control, limiting interpretation of the corresponding stained sample (Supplementary Fig. S1).

Supplementary Tables

Supplementary Table S1. Donor-level characteristics and assay participation

Characteristics and assay participation are listed for the clinical cohort (HC01–HC04 and TRD01–TRD07) and one additional ineligible participant. HC04 and TRD04 contributed clinical data only. HC01 and HC02 underwent exploratory panoptic assessment under control, LPS, LPS + DMT, and LPS + HRM conditions. The principal pharmacological assays used TRD-derived cells. Assay participation varied with differentiation success, sample yield, and processing priority; biological sample sizes are reported for each analysis.

Code	Group	Sex	Age (y)	Illness duration (y)	MADRS total	Concomitant medication	Assays contributed
HC01	HC	F	46	—	3	Yes	Panoptic morphology
HC02	HC	F	37	—	5	No	Cytometry (CD11b/CD45), Panoptic morphology
HC03	HC	F	33	—	4	Yes	Cytometry (CD11b/CD45)
HC04	HC	M	28	—	2	No	Excluded from cellular assays (data error)
TRD01	TRD	M	26	8	41	Yes	HCI
TRD02	TRD	M	26	1	43	Yes	Cytometry (CD11b, CD45, CD86, PI), HCI, AFM
TRD03	TRD	M	52	8	46	Yes	Cytometry (TMEM119, CD86, CD200, CD11b, CD45, PI), RT-qPCR (IL6, IL10, TNF, TGFB1), HCI, AFM
TRD04	TRD	M	27	10	35	Yes	No iMG differentiation; excluded from cellular assays
TRD05	TRD	F	45	2	32	Yes	Cytometry (CD200, CD86), RT-qPCR (IL6, IL10, TNF, TGFB1)
TRD06	TRD	F	54	9	40	Yes	Cytometry (PI, CD200, CD86), RT-qPCR (IL6, IL10, TNF, TGFB1)
TRD07	TRD	M	21	7	45	Yes	Cytometry (PI, CD200, CD86), RT-qPCR (IL6, IL10, TNF, TGFB1)
TRD-excl-B	Ineligible for TRD	M	34	0.5	20	Yes	None (sample frozen, unused)

HC, healthy control; TRD, treatment-resistant depression; MADRS, Montgomery–Åsberg Depression Rating Scale; HCI, high-content imaging; AFM, atomic force microscopy; PI, propidium iodide. TRD04 was excluded from cellular assays because the cells failed to acquire the adherent, process-bearing morphology expected after iMG differentiation. Instead, they remained rounded and suspended, resembling their appearance at initial plating. This participant was retained in the clinical characterization. HC04 also contributed clinical data but was excluded from cellular assays because of a data-collection error. TRD-excl-B did not meet the eligibility criteria for TRD. Donor numbering reflects the recruited cohort. For RT-qPCR, four donor observations were available in each condition for *IL10*, *TNF*, and *TGFB1*. *IL6* had four observations in control, LPS, and LPS + DMT and three in LPS + HRM. Missing expression values were not imputed.

Supplementary Table S2. Estimated half-maximal inhibitory concentrations obtained in the cytotoxicity screening assays

Cell type	Compound	24 h IC_{50} (95% CI)	48 h IC_{50} (95% CI)	72 h IC_{50} (95% CI)	Selected iMG concentration
Astrocytes	DMT	259.0 µg/mL (185.4–397.5)	216.6 µg/mL (180.6–262.9)	255.6 µg/mL (198.8–341.8)	90 µg/mL
Astrocytes	HRM	112.5 µM (110.0–122.2)	84.71 µM (70.98–100.6)	ND	35 µM
PBMCs	DMT	184.9 µg/mL (167.1–203.8)	ND	ND	—
PBMCs	HRM	112.6 µM (83.17–164.4)	ND	ND	—

Data were obtained by nonlinear regression from three independent experiments performed in duplicate. CI, confidence interval; DMT, N,N-dimethyltryptamine; HRM, harmine; iMG, monocyte-derived microglia-like cell; ND, not determined; PBMC, peripheral blood mononuclear cell.

Supplementary Table S3. Primer sequences used for RT-qPCR

Gene	Forward primer (5′–3′)	Reverse primer (5′–3′)
ACTB	CGCGAGAAGATGACCCAG	TAGCACAGCCTGGATAGCAA
GAPDH	GGAGCGAGATCCCTCCAAAAT	GGCTGTTGTCATACTTCTCATGG
IL10	GGTGATGCCCCAAGCTGAGA	AGATGCCTTTCTCTTGGAGCTTAT
IL6	TACCCCCAGGAGAAGATTCC	TTTCTGCCAGTGCCTCTTT
TNF	CCTGCTGCACTTTGGAGTGA	GATGAGGTACAGGCCCTCTG
TGFB1	TACCTGAACCCGTGTTGCTC	CCGGTAGTGAACCCGTTGAT

All sequences are written in the 5′–3′ direction. Primers were used at a final concentration of 500 nM. ACTB and GAPDH served as reference genes. TNF and TGFB1 correspond to the TNFα and TGFβ labels used in the figures.

Supplementary Table S4. Clinical characteristics of the final study cohort.

Variable	Healthy controls (n = 4)	TRD (n = 7)	Statistical test	p value
Age, years	36.00 ± 7.62	35.86 ± 13.95	Exact permutation Mann-Whitney U = 17	0.6121
Sex, female/male	3/1	2/5	Fisher's exact test	0.2424
MADRS total score	3.50 ± 1.29	40.29 ± 5.15	Exact permutation Mann-Whitney U = 0	0.0061
Family psychiatric history, yes/no	2/2	2/5	Fisher's exact test	0.5758
Illness duration, years	Not applicable	6.43 ± 3.51	Descriptive	Not applicable

Data are mean ± standard deviation or counts, as appropriate. TRD, treatment-resistant depression; MADRS, Montgomery-Åsberg Depression Rating Scale.

Supplementary Table S5. Concentration-selection screens and working concentrations used in iMG experiments.

Compound	Screening range	Screening exposure duration	Working concentration in iMGs	iMG exposure protocol	Interpretation
DMT	0.78–800 µg/mL	24, 48, and 72 h	90 µg/mL	3 h after 24 h LPS challenge	Selected from preliminary viability screening; not intended to reproduce clinically relevant exposure
Harmine	1.56–200 µM	24 and 48 h	35 µM	3 h after 24 h LPS challenge	Selected from preliminary viability screening; not interpreted as defining a microglia-specific therapeutic window
LPS	Not applicable	Not applicable	100 ng/mL	24 h before DMT or harmine	Used to establish an LPS-evoked inflammatory response before pharmacological treatment

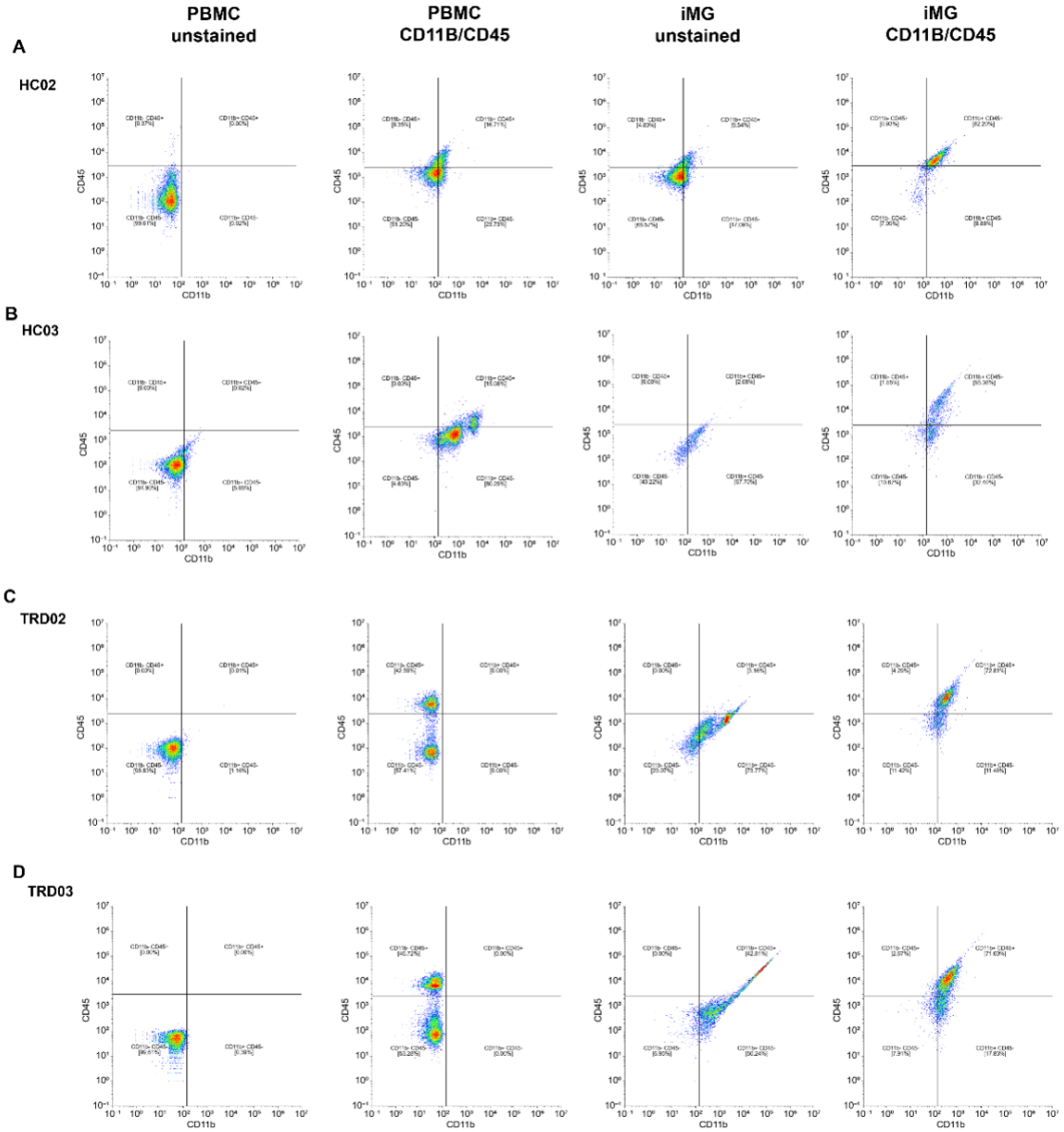
DMT, N ,N-dimethyltryptamine; HRM, harmine; iMG, monocyte-derived microglia-like cell; LPS, lipopolysaccharide. Screening assays were used only to guide working-concentration selection. They were not interpreted as establishing absence of treatment-related toxicity, microglia-specific safety, target selectivity, or clinically relevant exposure ranges.

Supplementary Table S6. Surface-marker positivity across experimental conditions.

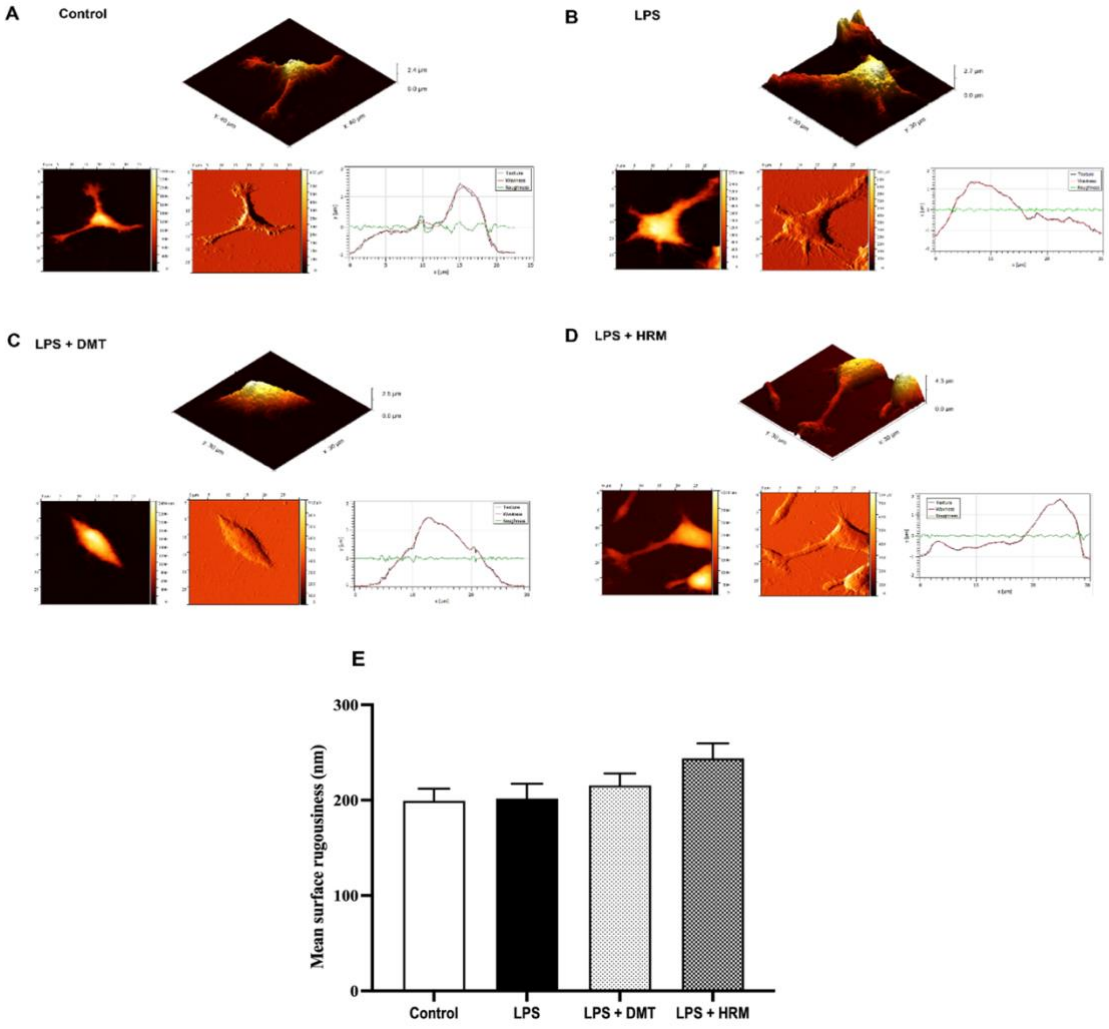
Marker	n donors	Control	LPS	LPS + DMT	LPS + HRM	Global test	p value
TMEM119-positive cells (%)	1	52.48	20.84	27.93	29.03	Descriptive	Not applicable
CD86-positive cells (%)	4	90.82 ± 4.09	90.41 ± 4.60	88.88 ± 4.19	90.30 ± 5.64	Friedman $\chi^2 = 2.85$	0.416
CD200-positive cells (%)	4	81.66 ± 10.39	82.84 ± 11.98	80.52 ± 10.63	85.56 ± 8.14	Friedman $\chi^2 = 1.20$	0.753

Values are percentages or mean ± standard deviation. Surface-marker outcomes quantify the fraction of positive cells and do not measure fluorescence intensity. DMT, N,N-dimethyltryptamine; HRM, harmine; LPS, lipopolysaccharide.

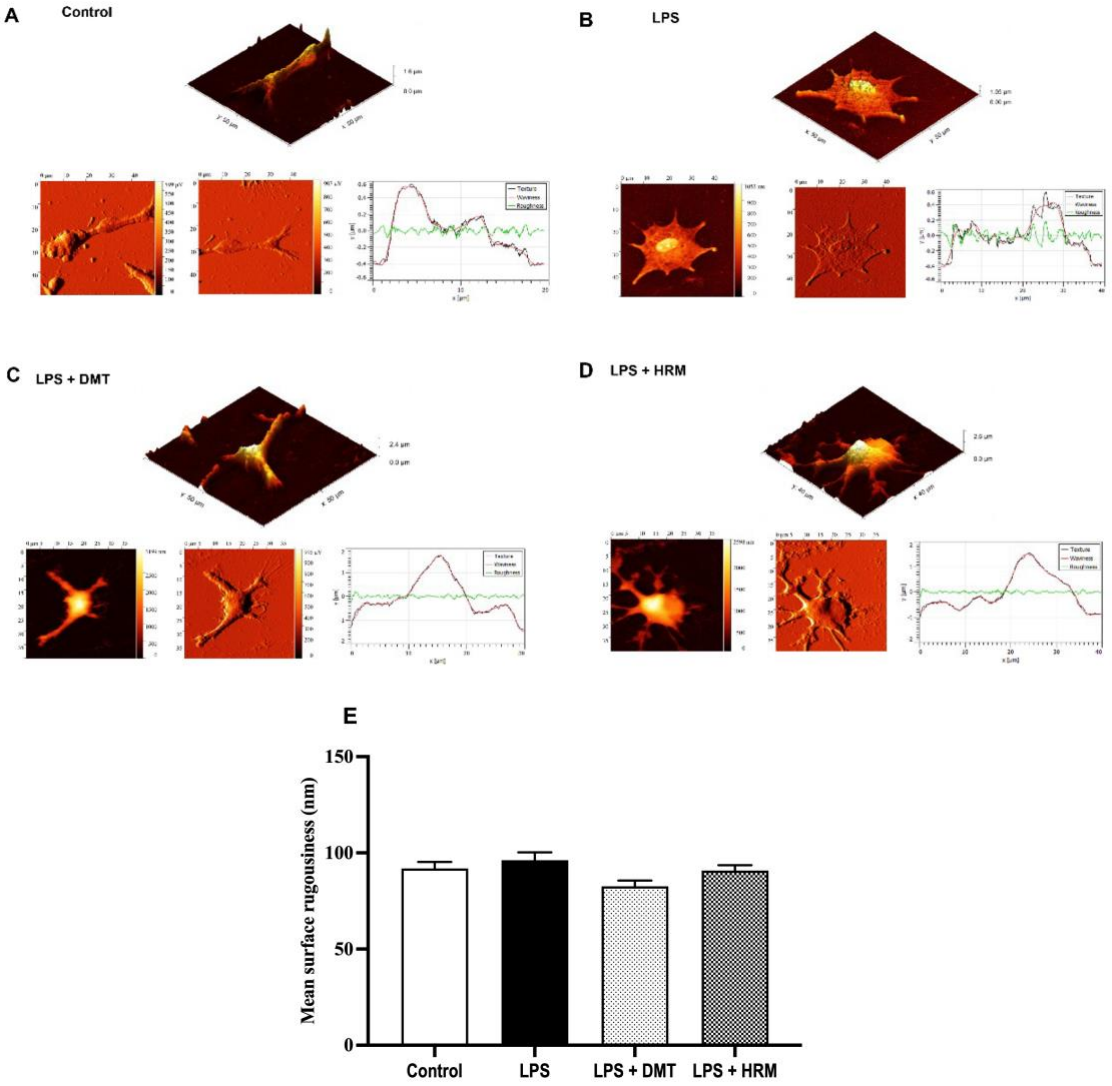
Supplementary Fig. S1. Representative CD11b/CD45 flow cytometry dot plots of PBMCs and monocyte-derived microglia-like cells (iMGs). Representative CD11b versus CD45 dot plots from (A) HC02, (B) HC03, (C) TRD02, and (D) TRD03. For each donor, plots are shown in the following order: unstained PBMCs, CD11b/CD45-stained PBMCs, unstained iMGs, and CD11b/CD45-stained iMGs. Quadrant gates indicate the relative distribution of $CD11b^{-}CD45^{-}$, $CD11b^{-}CD45^{+}$, $CD11b^{+}CD45^{-}$, and $CD11b^{+}CD45^{+}$ cell populations. Differentiated iMGs showed an increased proportion of $CD11b^{+}CD45^{+}$ cells compared with the corresponding PBMC populations, with donor-to-donor variability. Unstained controls are shown to document background fluorescence and support interpretation of marker-positive populations. The TRD03 unstained iMG sample exhibited substantial background signal in the $CD11b^{+}CD45^{+}$ quadrant and was therefore interpreted with caution. HC, healthy control; TRD, treatment-resistant depression; PBMCs, peripheral blood mononuclear cells; iMGs, monocyte-derived microglia-like cells.



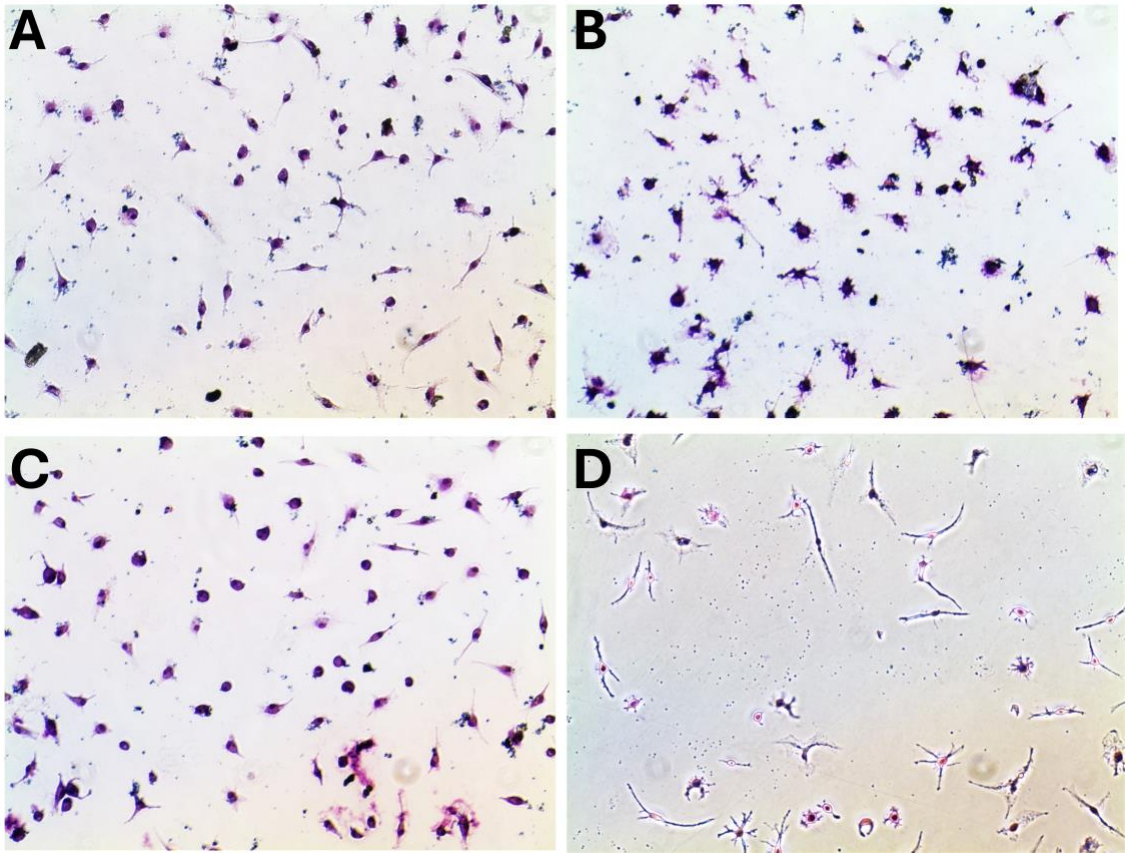
Supplementary Fig. S2. Exploratory atomic force microscopy analysis of iMGs derived from patient TRD02. Representative AFM images of iMGs under (A) control, (B) LPS, (C) LPS + DMT, and (D) LPS + HRM conditions. For each experimental condition, representative three-dimensional (3D) surface topography, two-dimensional (2D) height and amplitude images, and the corresponding surface profile showing texture, waviness, and roughness are presented. (E) Donor-specific mean surface roughness (Ra) across experimental conditions. Mean Ra values were 199.3 nm for control, 201.8 nm for LPS, 215.3 nm for LPS + DMT, and 243.9 nm for LPS + HRM. Roughness measurements were obtained from 60 regions per experimental condition within this donor and are presented descriptively as mean ± SEM; these measurements do not represent independent biological replicates. Accordingly, no population-level inferential conclusions were drawn from this donor-specific analysis. DMT, N,N-dimethyltryptamine; HRM, harmine; LPS, lipopolysaccharide; AFM, atomic force microscopy; iMGs, monocyte-derived microglia-like cells; Ra, average surface roughness.



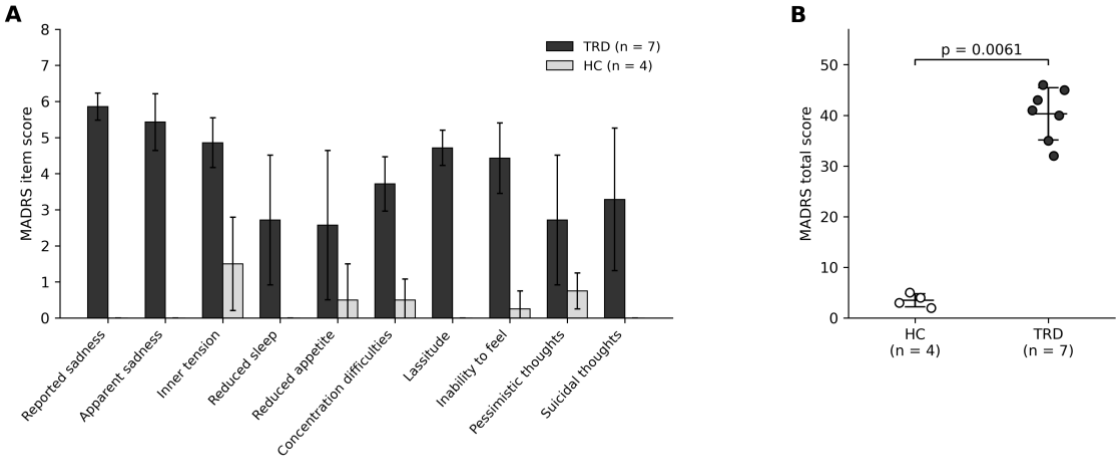
Supplementary Fig. S3. Exploratory atomic force microscopy analysis of iMGs derived from patient TRD03. Representative AFM images of iMGs under (A) control, (B) LPS, (C) LPS + DMT, and (D) LPS + HRM conditions. For each experimental condition, three-dimensional (3D) surface topography, two-dimensional (2D) height and amplitude images, and the corresponding surface profile showing texture, waviness, and roughness are presented. (E) Donor-specific mean surface roughness (Ra) across experimental conditions. Mean Ra values were 91.90 nm for control, 96.22 nm for LPS, 82.62 nm for LPS + DMT, and 90.79 nm for LPS + HRM after retaining all 130 analyzed regions per condition. Roughness measurements are presented descriptively as mean ± SEM; these measurements do not represent independent biological replicates. Accordingly, no population-level inferential conclusions were drawn from this donor-specific analysis. DMT, N,N-dimethyltryptamine; HRM, harmine; LPS, lipopolysaccharide; AFM, atomic force microscopy; iMGs, monocyte-derived microglia-like cells; Ra, average surface roughness.



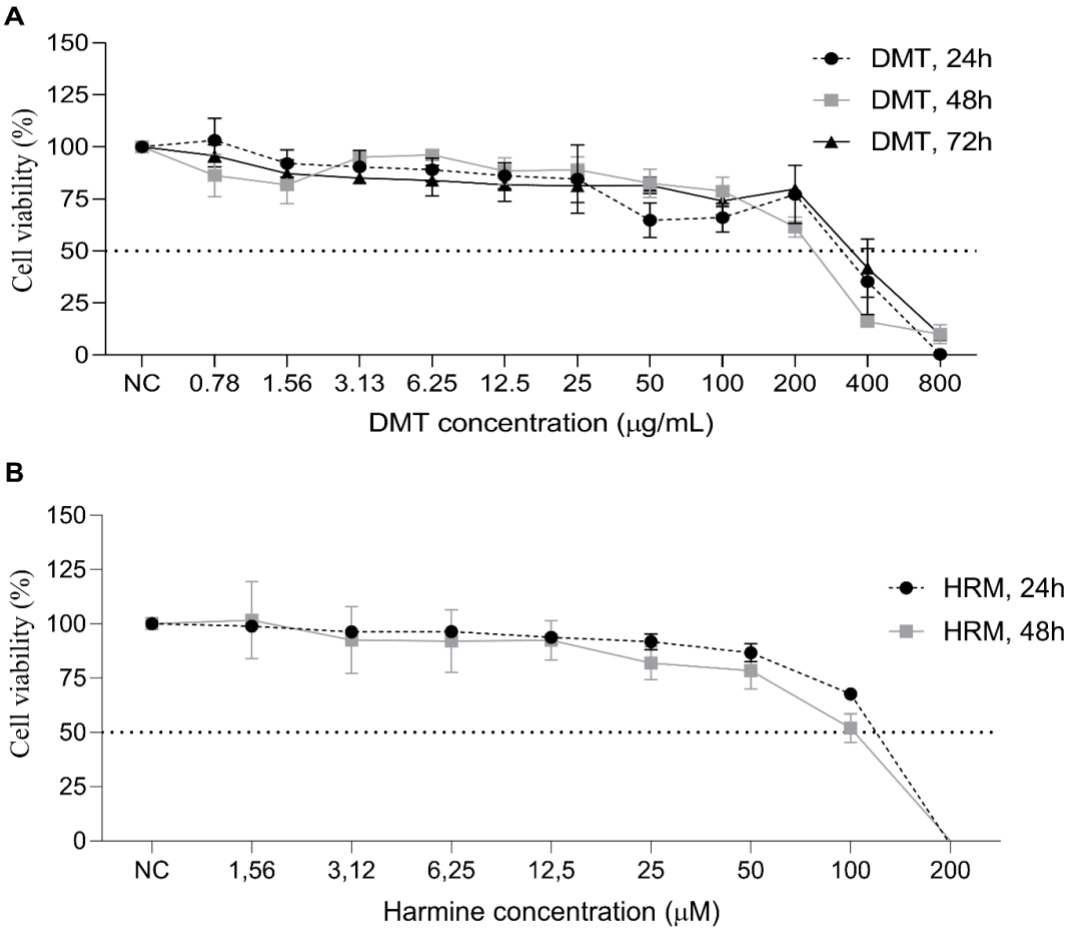
Supplementary Fig. S4. Panoptic-stained morphology of healthy-control-derived iMGs. Representative brightfield images from two healthy-control donors under (A) control, (B) LPS, (C) LPS + DMT, and (D) LPS + HRM conditions, acquired using a 20× objective. LPS-treated fields showed more rounded, less process-bearing profiles, whereas fields following DMT or HRM exposure showed more elongated profiles. These observations were descriptive; no cell-level inferential tests were performed. DMT, N,N-dimethyltryptamine; HRM, harmine; LPS, lipopolysaccharide.



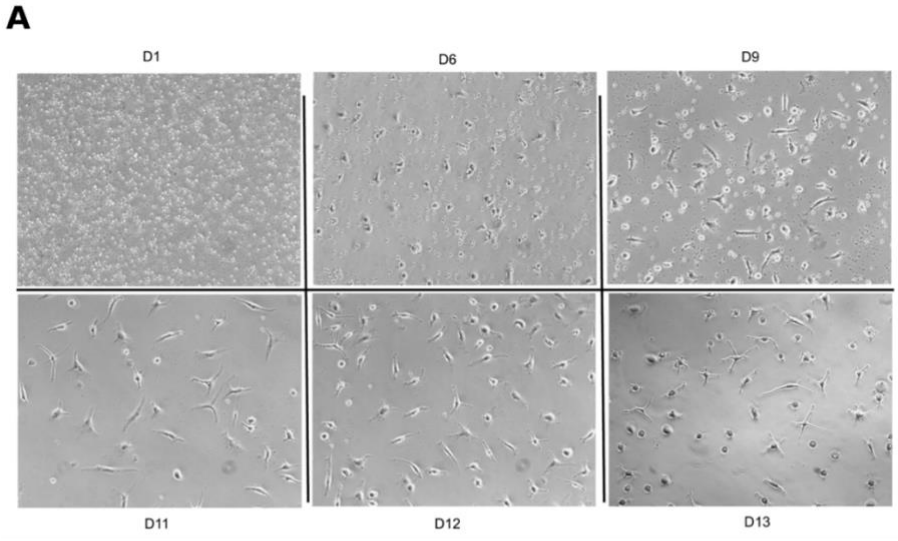
Supplementary Fig. S5. Clinical characterization of healthy controls and patients with treatment-resistant depression. (A) Mean scores for the ten Montgomery–Åsberg Depression Rating Scale (MADRS) items in healthy controls (HC, n = 4) and patients with treatment-resistant depression (TRD, n = 7). Bars show means and error bars show standard deviations. (B) Individual MADRS total scores; horizontal marks and error bars show means and standard deviations. Groups were compared using a two-sided Mann-Whitney U test with exhaustive permutation of group labels (U = 0, exact p = 0.0061). HC04 and TRD04 contribute to the clinical characterization despite their exclusion from cellular assays; TRD04 cultures failed to differentiate into iMGs.

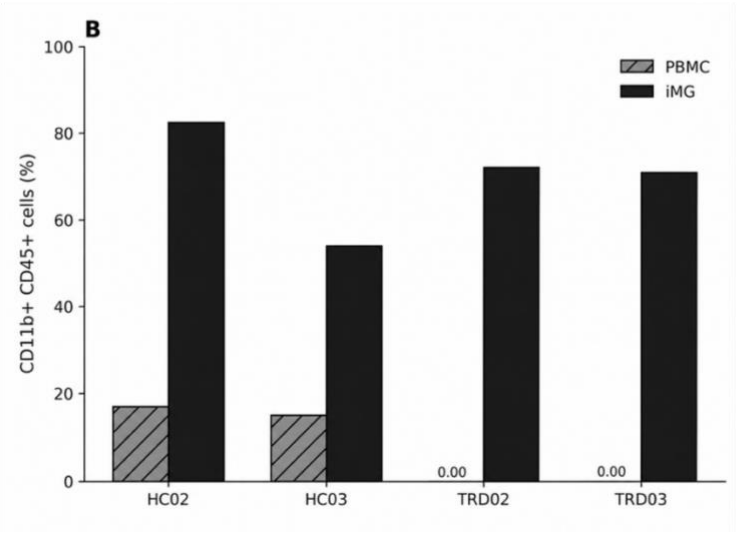


Supplementary Fig. S6. Concentration-dependent effects of N,N-dimethyltryptamine (DMT) and harmine (HRM) on astrocyte viability. (A) Cell viability following exposure to DMT (0.78 to 800 µg/mL) for 24, 48, and 72 h. (B) Cell viability following exposure to HRM (1.56 to 200 µM) for 24 and 48 h. NC denotes the untreated negative control. Cell viability was normalized to the untreated control and is expressed as a percentage of control. Symbols and error bars show mean ± standard deviation from three independent experiments performed in duplicate. The horizontal dotted line marks 50% cell viability, the reference used for half-maximal inhibitory concentration (IC50) estimation. Estimated IC50 values are reported in Supplementary Table S2; working concentrations are summarized in Supplementary Table S5. DMT (90 µg/mL) and HRM (35 µM) were selected for subsequent experiments with patient-derived microglia-like cells (iMGs).



Supplementary Fig. S7. Differentiation and phenotypic characterization of monocyte-derived microglia-like cells. (A) Representative brightfield images acquired on culture days 1, 6, 9, 11, 12, and 13, showing increasing adherence and process-bearing morphology. (B) Individual $CD11b^{+}CD45^{+}$ percentages in PBMCs and differentiated iMGs from HC02, HC03, TRD02, and TRD03. Measurements are descriptive; no inferential comparisons were performed. High background in the TRD03 no-antibody control limits interpretation of that donor's percentage. Representative plots and controls are provided in Supplementary Fig. S1.





Supplementary References

Bruzelius A, Hidalgo I, Boza-Serrano A, Hjelmér A-G, Tison A, Deierborg T et al (2021) The human bone marrow harbors a CD45− CD11B+ cell progenitor permitting rapid microglia-like cell derivative approaches. Stem Cells Transl Med 10:582–597. https://doi.org/10.1002/sctm.20-0127

Denizot F, Lang R (1986) Rapid colorimetric assay for cell growth and survival: modifications to the tetrazolium dye procedure giving improved sensitivity and reliability. J Immunol Methods 89:271–277. https://doi.org/10.1016/0022-1759(86)90368-6

Mosmann T (1983) Rapid colorimetric assay for cellular growth and survival: application to proliferation and cytotoxicity assays. J Immunol Methods 65:55–63. https://doi.org/10.1016/0022-1759(83)90303-4

O'Brien J, Wilson I, Orton T, Pognan F (2000) Investigation of the Alamar Blue (resazurin) fluorescent dye for the assessment of mammalian cell cytotoxicity. Eur J Biochem 267:5421–5426. https://doi.org/10.1046/j.1432-1327.2000.01606.x